POLİTEKNİK DERGİSİ

JOURNAL of POLYTECHNIC

ISSN: 1302-0900 (PRINT), ISSN: 2147-9429 (ONLINE)
URL: http://dergipark.org.tr/politeknik

Microstrip stub filter design with enhanced performance inspired by SIW structures operating at 1.93 GHz GSM band

1.93 GHz GSM bandında çalışan SIW yapılarından esinlenilmiş gelişmiş performansa sahip mikroşerit saplama filtre tasarımı

***Yazar(lar) (Author(s))**: Hüseyin TOSUN[1], Abdulkadir YENTÜR[2], Veli Tayfun KILIÇ[3]*

ORCID[1]: 0000-0001-8774-6240

ORCID[2]: 0000-0002-9828-929X

ORCID[3]: 0000-0001-6806-9053

To cite to this article: Tosun H., Yentür A., and Kılıç V. T., "Microstrip Stub Filter Design with Enhanced Performance Inspired by SIW Structures Operating at 1.93 GHz GSM Band", ***Journal of Polytechnic***, 29(3):290301:1-12 (2026).

Bu makaleye şu şekilde atıfta bulunabilirsiniz: Tosun H., Yentür A. ve Kılıç V. T., "Microstrip Stub Filter Design with Enhanced Performance Inspired by SIW Structures Operating at 1.93 GHz GSM Band", ***Politeknik Dergisi***, 29(3):290301:1-12 (2026).

Erişim linki (To link to this article): http://dergipark.org.tr/politeknik/archive

DOI: 10.2339/politeknik.1470601

Microstrip Stub Filter Design with Enhanced Performance Inspired By SIW Structures Operating at 1.93 GHz GSM Band

Highlights

- *Microstrip stub filter design operating at 1.93 GHz band*
- *Enhanced filter performance inspired by SIW structures*
- *Analysis of the designed filter with various numbers of additional vias and different via to microstrip line distances*
- *Production of the filters with and without additional vias and their performance measurements*
- *Construction of a receiver system with the manufactured filters and recording the signals in the system*

Graphical Abstract

In this study, a microstrip stub pass band filter with improved performance inspired by SIW structures operating at 1.93 GHz was designed.

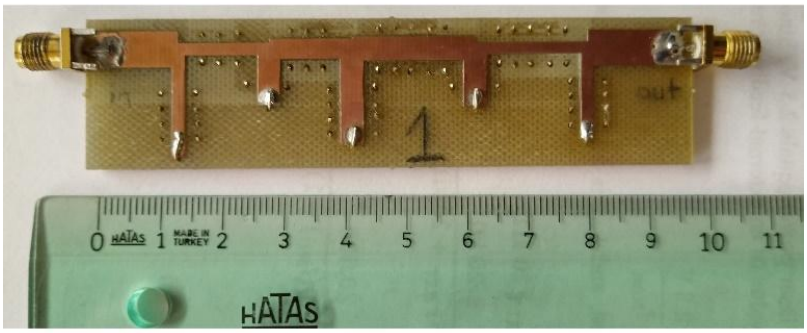

Figure. The manufactured filter with additional vias placed around the microstrip lines.

Aim

To improve microstrip stub filter perfromance by applying SIW structure and analyze the changes in the filter behaviour with numbers and distances of added vias.

Design & Methodology

3D EM simulations were obtained for the designed filter with different numbers of additional vias and various via to microstrip line distances. After, the designed filters were produced and their transmission responses were measured. Also, system experiments were performed with a receiver system at 1.93 GHz.

Originality

Optimum filter design has been achieved with 3D EM simulations after systematic changes of the parameter. The EM waves propagating through the filter is enclosed more and the transmission loss of the filter in the pass band is lowered.

Findings

The maximum transmission coefficient, i.e., S_{21} parameter, magnitude value reached in the pass band of the filter increases, while the frequency at which the peak S_{21} parameter value is achieved shifts to lower frequencies as the number of the vias around the microstrip lines increases and the distance between the vias and the lines decreases.

Conclusion

By applying SIW structure performance of the designed micrsotrip stub filter operating at 1.93 GHz GSM band has been improved. The proposed filter architecture is promising for applications requiring high signal-to-noise ratio.

Declaration of Ethical Standards

The authors of this article declare that the materials and methods used in this study do not require ethical committee permission and/or legal-special permission.

Microstrip Stub Filter Design with Enhanced Performance Inspired By SIW Structures Operating at 1.93 GHz GSM Band

Araştırma Makalesi / Research Article

Hüseyin TOSUN[1*], Abdulkadir YENTÜR[2], Veli Tayfun KILIÇ[1]

[1]Department of Electrical and Electronics Engineering, Abdullah Gül University, Türkiye
[2]Department of Electrical and Electronics Engineering, TOBB University of Economics and Technology, Türkiye

(Received/Geliş : 06.05.2024 ; Accepted/Kabul : 11.01.2025 ; Early View/Erken Görünüm : 14.10.2025)

ABSTRACT

This paper reports a microstrip stub filter design operating at 1.93 GHz GSM band with enhanced performance inspired by SIW structures. In the designed filter additional vias are placed around the microstrip lines to enhance the encasing of the electromagnetic fields while propagating through the filter to develop the filter performance. The filter was examined with electromagnetic simulations for various numbers of vias and different via to microstrip line distances. Results show that the maximum transmission coefficient (S_{21} parameter) magnitude value reached in the pass band of the filter increases with the number of the vias and as the vias get closer to the lines. On the other hand, when the via number increases and the space between them and the lines narrows, the frequency at which the maximum S_{21} value is attained shifts to lower frequencies. The designed filters were manufactured, too. Results obtained in the measurements agree well with the simulation results. Additionally, a receiver system operating at 1.93 GHz band was constructed. System experiments were carried out with the constructed prototype for the manufactured filters. Results show that a greater signal level in the filter pass band is achieved and unwanted signals outside the filter pass band are suppressed more in the system where the filter with vias is used instead of the filter without any additional via. The findings indicate that the designed filters inspired by SIW structures are promising for applications requiring high signal quality.

Keywords: Microstrip band-pass filter, SIW structure, 1.9 GHz GSM band.

1.93 GHz GSM Bandında Çalışan SIW Yapılarından Esinlenilmiş Gelişmiş Performansa Sahip Mikroşerit Saplama Filtre Tasarımı

ÖZ

Bu makale SIW yapılarından esinlenilerek gelişmiş performansa sahip 1.93 GHz GSM bandında çalışan bir mikroşerit saplamalı filtre tasarımını sunmaktadır. Tasarlanan filtrede elektromanyetik alanların filtre içerisinde ilerlerken kapsanmasını arttırmak için mikroşerit hatların etrafına ek toprak bağlantı geçişleri yerleştirilmiştir. Filtre, çeşitli sayıdaki geçişler ve farklı geçiş-mikroşerit hat mesafeleri için elektromanyetik simülasyonlarla incelenmiştir. Sonuçlar, filtrenin geçirgen bandında ulaşılan maksimum iletim katsayısı (S_{21} parametresi) büyüklük değerinin geçiş sayısı arttıkça ve geçişler hatlara yaklaştıkça arttığını göstermektedir. Öte yandan, geçiş sayısı arttığında ve hatlarla aralarındaki mesafe daraldığında maksimum S_{21} değerinin ulaşıldığı frekans daha düşük frekanslara kaymaktadır. Tasarlanan filtrelerin üretimi de gerçekleştirildi. Ölçümlerde elde edilen sonuçlar simülasyon sonuçlarıyla oldukça uyumludur. Ayrıca, 1.93 GHz bandında çalışan alıcı sistemi inşa edilmiştir. Üretilen filtreler için oluşturulan prototip ile sistem deneyleri gerçekleştirilmiştir. Sonuçlar, herhangi bir ek toprak bağlantı geçişi bulunmayan filtre yerine, geçişlerin olduğu filtrenin kullanıldığı sistemde, filtre geçirgen bandında daha yüksek bir sinyal seviyesine ulaşıldığını ve filtre geçirgen bandı dışındaki istenmeyen sinyallerin daha fazla bastırıldığını göstermektedir. Bulgular, SIW yapılarından esinlenerek tasarlanan filtrelerin yüksek sinyal kalitesi gerektiren uygulamalar için umut verici olduğunu göstermektedir.

Anahtar Kelimeler: Mikroşerit bantgeçiren filtre, SIW yapısı, 1.9 GHz GSM bandı.

1. INTRODUCTION

A filter is a circuit device that permits signals at certain frequencies to pass while suppressing the others. Filters are commonly used in many electrical applications, such as power supplies, audio electronics, ADC's and radio communications [1, 2]. Although a simple filter can be designed by using components like resistors, capacitors and inductors, lumped circuit theories mostly become invalid for microwave devices due to their high operating frequencies [3]. Microstrip structures are commonly used at microwave frequencies thanks to their advantages including simple construction, having small sizes and high reliability [4-7].

RF filters have very wide variety of usages including biomedical signal processing [8, 9], Wi-Fi networks [10, 11], satellite communications [12-14], etc. Another

*Sorumlu Yazar (Corresponding Author)
e-posta : huseyin.tosun@agu.edu.tr

application in which RF filters are required is GSM (Global System for Mobile) communication systems [15, 16]. GSM is a digital network commonly used for a mobile phone communication [17, 18]. There are different generations of GSM networks and each generation operates at different frequencies depending on the region. For instance, 900 MHz and 1800 MHz bands are used in European, Asian and African countries in the second and third generation, i.e., 2G and 3G, networks, whereas in north America 850 MHz and 1900 MHz bands are used in 2G and 3G networks [19].

Signal quality is an important parameter in GSM communications. Since the communication is achieved at very far distances, signal level received by the antennas is very small. For example, signal level reached to a cell phone at the 2G frequency band is around -70 dBm, i.e., 10^{-10} W [20]. Also, noise signals exist in an environment decrease the received signal quality. Moreover, reflections, refractions, and scattering of the signal affect system performance. To enhance received power and system performance antennas with different structures operating at certain frequency bands depending on the generation of the communication system were developed [21-24] and propagation channel characteristics were investigated [25-27]. However, in addition to antenna developments and channel optimizations, in the receiver circuitry of a GSM system it is required to pass the signals carrying the information with a minimum loss while maximally suppressing the unwanted noise signals exist in the rest of the frequency spectrum.

There are different RF filter designs in literature proposed for high quality received signals. For instance, surface acoustic wave (SAW) filters [28, 29], cavity filters [30-32] and planar filters [33-35] are some of the common filter types used for better selectivity and higher stability in a frequency spectrum. As different from those filter designs, in this study RF microstrip stub filter inspired by substrate integrated waveguide (SIW) structures is introduced. SIW structures were used in literature works especially in transmission lines [36-39], couplers [40-43], power dividers [44-47] and antennas [48-51]. In addition, there are studies about SIW based filters [52-54]. In these filters different design approaches were applied. For instance, half mode SIW band pass filter [52, 53] and a SIW filter with an arrow pattern vias [54] were investigated. In these designs to improve filter performance different SIW geometries were used. However, in some other literature works SIW filtering is combined with other techniques [55-57]. In [55] corrugated structures and periodic slots are added on a SIW based band pass filter, whereas in [56] gradient and periodic slots are placed to a half mode SIW band pass filter. Also, a hybrid structure band pass filter in which microstrip impedance resonators are etched between two SIW cavities was investigated, too [57]. In the proposed structure 8-like shape microstrip impedance resonators prevent coupling between SIW cavities at high frequencies. Apart from these studies, a hybrid microstrip-SIW band pass filter was reported in [58]. Here, in the design a SIW high pass filter is cascaded by a low pass stepped-impedance filter.

Different from what is reported in the literature, in this study, the SIW structure is applied to a microstrip stub band pass filter for a performance enhancement. With simulations an optimum filter design was obtained and the prototype was fabricated. Simulations and measurement results demonstrate the performance increase of the designed stub filter with utilization of the SIW structure. Also, experiments were obtained with an RF receiver system operating at 1.93 GHz GSM band. Results verify the system performance increase and the signal quality enhancement by employing the designed filter.

2. FILTER DESIGN and ANALYSIS

A microstrip stub filter operating in the 1.86 GHz–2.0 GHz pass band was initially designed. The filter consists of shorted stubs separated with microstrip lines. These filter structures were reported before in literature for different applications [59]. The center frequency of the designed filter pass band is set to 1.93 GHz, so the filter allows GSM signals around 1.93 GHz at a high level. Circuit schematic of a filter with shorted stubs separated by microstrip lines is shown in Fig. 1.

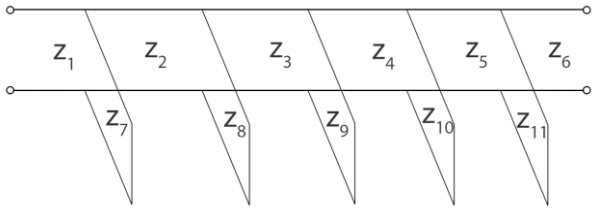

Figure 1. Circuit schematic of a filter with shorted stubs separated by microstrip lines

As seen, in the filter there are 5 shorted stubs separated with 4 microstrip lines between. In the figure characteristic impedances of the lines are indicated with Z_1, Z_2, Z_3, Z_4, Z_5, Z_6, Z_7, Z_8, Z_9, Z_{10} and Z_{11}. One can compute a microstrip line's characteristic impedance by using (1) if its geometrical parameters and electrical properties of its material are known [3].

$$Z_i = \begin{cases} \frac{60}{\sqrt{\epsilon_e}} \ln\left(\frac{8t_s}{W} + \frac{W}{4t_s}\right), \text{for } W/t_s \le 1 \\ \frac{120\pi}{\sqrt{\epsilon_e}[W/t_s + 1.393 + 0.667\ln(W/t_s + 1.444)]}, \text{for } W/t_s \ge 1 \end{cases} \quad (1)$$

In the equation Z_i represents characteristic impedances of the lines. In the designed filter i can be 1, 2, 3, …, 11, since there are 11 microstrip lines in total. Also, W and t_s are width of the transmission line and separation between the top and bottom layers, i.e., substrate material thickness, in the line, respectively. In addition, ϵ_e stands for the line's effective dielectric constant

formulated as in (2), where $\in_r$ represents relative permittivity of the substrate material.

$$\in_e = \frac{\in_r+1}{2} + \frac{\in_r-1}{2}\frac{1}{\sqrt{1+12t_s/W}} \quad (2)$$

For a known reference impedance by applying impedance transformations equivalent impedance seen at the input side of the filter together with the S parameters can be calculated, where the transmission lines are assumed to be lossless. For this, initially, equivalent impedances seen at the input terminals of the shorted vertical microstrip lines are formulated as in (3)

$$Z_m' = Z_m \frac{Z_L + jZ_m \tan(\beta_m h_k)}{Z_m + jZ_L \tan(\beta_m h_k)} \xrightarrow[Z_L=0]{} Z_m' = jZ_m \tan(\beta_m h_k) \quad (3)$$

,where Z_m' is the observed impedance at the input terminals of the shorted vertical microstrip line having characteristic impedance of Z_m, i.e., m = 7, 8, 9, 10, and 11 (see Figs. 1 and 2). On the other hand, h_k is the length of the corresponding microstrip line, i.e., k = 1, 2, 3, 4, and 5 (see Fig. 2). In addition, Z_L represents the load impedance, whose value is 0 because of short ending of the lines. In the equation, β_m is the propagation constant of a wave inside the corresponding line and it is expressed as

$$\beta = \frac{2\pi}{\lambda} \quad (4)$$

$$\lambda = \frac{c}{f\sqrt{\in_e}} \quad (5)$$

,where λ and f are the wavelength and the frequency, respectively, and c is the speed of a wave in free-space. In the calculations wave velocity in free-space (c) is taken to be 2.99792458×10^8 (m/s). It is important to note that the effective dielectric constant ($\in_e$) of each microstrip line in the filter might be different depending on its width (W) (see equation (2)) and thus the wavelength (λ) and the propagation constant (β) might be different, too.

After, equivalent impedances seen at the input terminals of the horizontal microstrip lines can be calculated starting from the load side and ending at the input side as follows.

$$Z_{load1} = \left(Z_6 \frac{Z_{ref} + jZ_6 \tan(\beta_6 l_6)}{Z_6 + jZ_{ref} \tan(\beta_6 l_6)}\right) // Z_{11}' = \frac{1}{\left(\frac{1}{Z_6 \frac{Z_{ref} + jZ_6 \tan(\beta_6 l_6)}{Z_6 + jZ_{ref} \tan(\beta_6 l_6)}}\right) + \frac{1}{Z_{11}'}} \quad (6a)$$

$$Z_{load2} = \left(Z_5 \frac{Z_{load1} + jZ_5 \tan(\beta_5 l_5)}{Z_5 + jZ_{load1} \tan(\beta_5 l_5)}\right) // Z_{10}' = \frac{1}{\left(\frac{1}{Z_5 \frac{Z_{load1} + jZ_5 \tan(\beta_5 l_5)}{Z_5 + jZ_{load1} \tan(\beta_5 l_5)}}\right) + \frac{1}{Z_{10}'}} \quad (6b)$$

$$Z_{load3} = \left(Z_4 \frac{Z_{load2} + jZ_4 \tan(\beta_4 l_4)}{Z_4 + jZ_{load2} \tan(\beta_4 l_4)}\right) // Z_9' = \frac{1}{\left(\frac{1}{Z_4 \frac{Z_{load2} + jZ_4 \tan(\beta_4 l_4)}{Z_4 + jZ_{load2} \tan(\beta_4 l_4)}}\right) + \frac{1}{Z_9'}} \quad (6c)$$

$$Z_{load4} = \left(Z_3 \frac{Z_{load3} + jZ_3 \tan(\beta_3 l_3)}{Z_3 + jZ_{load3} \tan(\beta_3 l_3)}\right) // Z_8' = \frac{1}{\left(\frac{1}{Z_3 \frac{Z_{load3} + jZ_3 \tan(\beta_3 l_3)}{Z_3 + jZ_{load3} \tan(\beta_3 l_3)}}\right) + \frac{1}{Z_8'}} \quad (6d)$$

$$Z_{load5} = \left(Z_2 \frac{Z_{load4} + jZ_2 \tan(\beta_2 l_2)}{Z_2 + jZ_{load4} \tan(\beta_2 l_2)}\right) // Z_7' = \frac{1}{\left(\frac{1}{Z_2 \frac{Z_{load4} + jZ_2 \tan(\beta_2 l_2)}{Z_2 + jZ_{load4} \tan(\beta_2 l_2)}}\right) + \frac{1}{Z_7'}} \quad (6e)$$

$$Z_{in} = Z_1 \frac{Z_{load5} + jZ_1 \tan(\beta_1 l_1)}{Z_1 + jZ_{load5} \tan(\beta_1 l_1)} \quad (6f)$$

In the equations, // sign indicates parallel connection. Also, Z_{load1}, Z_{load2}, Z_{load3}, Z_{load4}, Z_{load5} are the equivalent impedances seen at the input terminals of the horizontal microstrip lines and Z_{in} is the filter's equivalent input impedance.

Lastly, S_{21} parameter of the filter is expressed as a function of the equivalent input impedance of the filter and the reference impedance by (7).

$$S_{21}(\text{dB}) = 20\log_{10}\left(\sqrt{1 - \left|\frac{Z_{in} - Z_{ref}}{Z_{in} - Z_{ref}}\right|^2}\right) \quad (7)$$

The equivalent impedances of the lines at their input sides and their lengths together with the reference impedance at the load end and characteristic impedances of the lines are represented in Fig. 2. As it is seen, the same symbols are used in the figure and the equations.

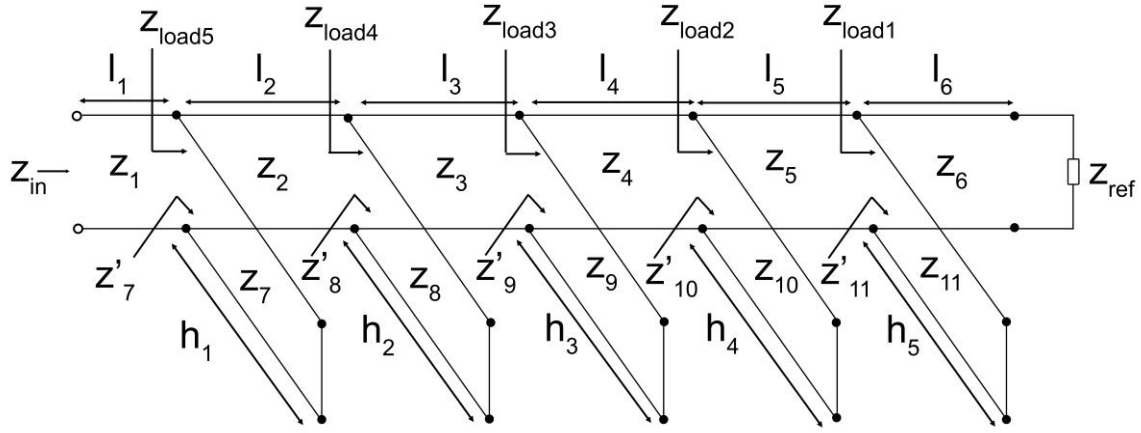

Figure 2. Circuit schematic of the filter with equivalent input impedances, line lengths, the reference impedance and characteristic impedances of the lines

In addition to analytical investigation, with help of an electromagnetic simulation tool the filter was modeled, too. An FR4 substrate is sandwiched between two copper layers in the modeled filter. The substrate and the copper layers have 1.53 mm and 0.035 mm thickness, respectively. The modeled filter structure is shown in Fig. 3 from side and top views. In the figure yellow regions show the copper material and green areas represent FR4. The thickness of the copper layers and the substrate material thickness are labeled with t_c and t_s, respectively, in Fig. 3(a). In Fig. 3(b), on the other hand, the width and length of the horizontal lines on the top are designated with letters w and l, respectively. Similarly, the width and length of the vertical microstrip lines, i.e., stubs, are labeled with letters s and h, respectively. Those labels were selected in harmony with the parameters used in the equations. In the figure, shorting vias at the end of the stubs are seen as circles. The modeled filter was optimized with simulations. Following the optimization, the geometrical parameters of the modeled filter are given in Table 1.

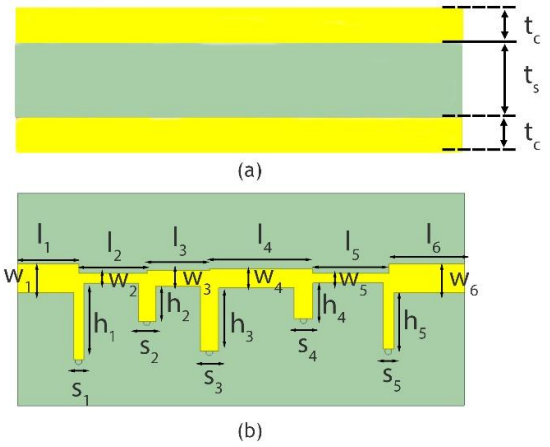

Figure 3. The filter structure modeled in simulations from (a) side and (b) top views

2.1. Filter Design with Increased Number of Vias

After optimization, to improve the filter performance additional vias are placed around the microstrip lines. In the simulations, the vias inserted around the microstrip lines are filled with a conductor made of Solder Alloy 99c material so that they are in contact with the bottom ground plate. By this way, it is aimed to enclose the electromagnetic waves propagating through the filter more and decrease the loss occurs due to fringing fields. Therefore, the transmission loss of the filter in the pass band is intended to be lowered.

Simulations were performed with different number of vias placed around the microstrip lines. The vias have the same geometry with those exist at the end of the stubs in the initially designed filter such that the vias have a cylindrical geometry with 1.4 mm diameter.

Table 1. Geometrical parameters of the filter

Parameter	Value (mm)	Parameter	Value (mm)
l_1	13.10	w_1	6.00
l_2	11.50	w_2	2.10
l_3	11.35	w_3	3.40
l_4	17.95	w_4	4.00
l_5	17.00	w_5	2.00
l_6	16.10	w_6	6.00
h_1	18.25	s_1	2.20
h_2	10.25	s_2	3.70
h_3	17.10	s_3	3.90
h_4	10.50	s_4	4.00
h_5	16.00	s_5	2.00
t_c	0.035	T_s	1.60

Also, the distance between a via and a copper line in the designed filter were set constant. The center points of the vias are 1 mm away from the copper line edges that are closest to the vias. In other words, the distance between the closest points of the vias and the nearest edges of the microstrip lines is 0.3 mm (1.0 mm – (1.4 mm / 2)). Top view of the filter design with various numbers of vias is given in Fig. 4.

2.2. Parametric Sweep of Via Distance

Later, simulations were repeated with the designed filter for different distances between the newly added vias and the copper lines. Throughout the analysis, the number of vias and their geometries remained unchanged while the distance between the lines and vias changed. By this way, effect of the proximity of the vias to the microstrip lines on the filter performance is investigated. In total there are 60 vias added to the initially designed stub filter and they have a cylindrical geometry with a circular cross section of 1.4 mm diameter. In the simulations, the distance between the vias and the microstrip lines changes from 0.1 mm to 1.0 mm with an increment of 0.1 mm. The distance between the newly added vias and the lines is pointed out and labeled with letter d in Fig. 5, where top view of the modeled filter geometry with 60 additional vias around the lines is represented.

3. RESULTS and DISCUSSION

Analytical calculations were done and simulations were started with the initially designed microstrip stub filter (see Fig. 1, Fig. 2 and Fig. 3). As previously stated, five shorting vias exist at the ends of the stubs and except these there is no additional via placed around the microstrip lines. The filter is optimized and has geometrical parameters given in Table 1. The footprint of the filter is 87 mm×25 mm. In the calculations and simulations reference impedance (Z_{ref}) is set to be 50

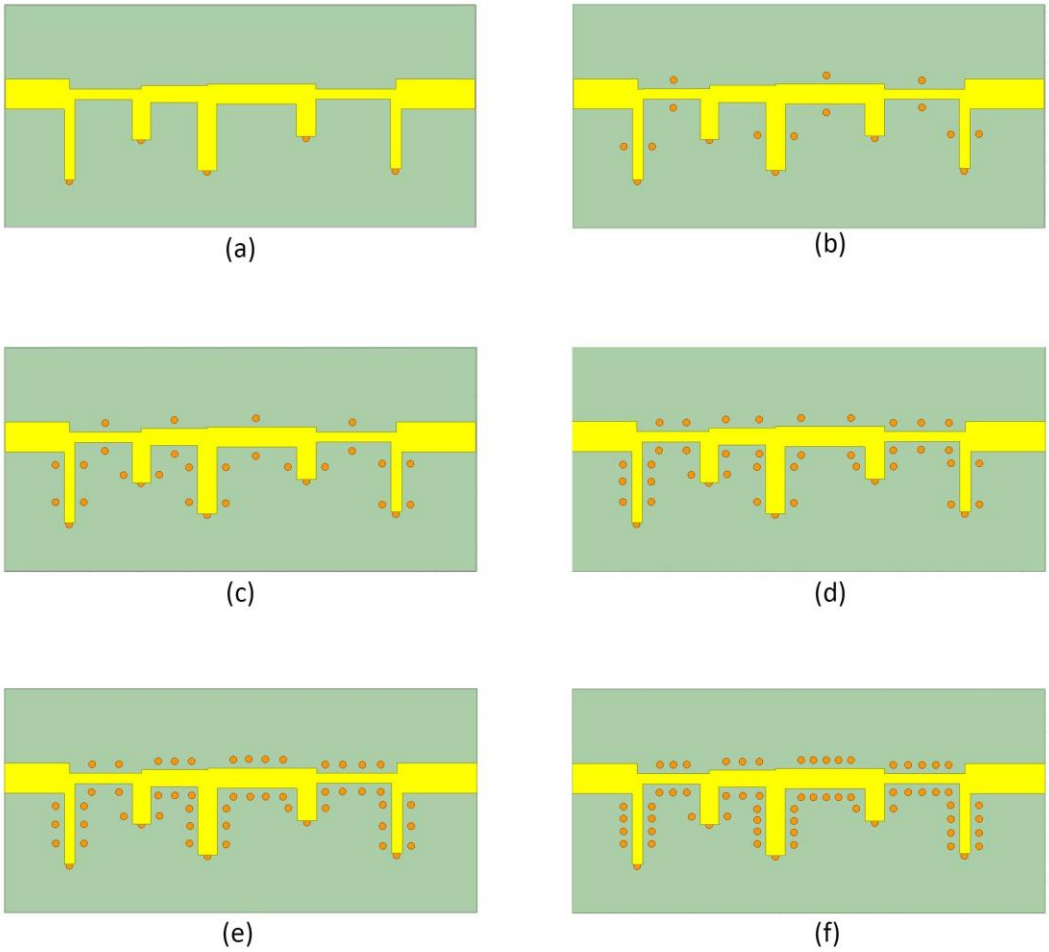

Figure 4. Top view of the designed filters. (a) Initially designed filter with no additional via, (b) - (f) filter designs with 12, 24, 36, 48 and 60 additional vias around the microstrip lines

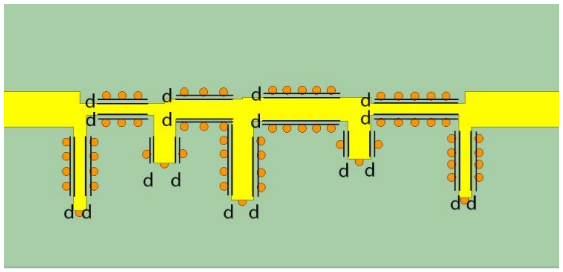

Figure 5. Top view of the designed filter with 60 additional vias, where distance between the added vias and the lines is labeled as d

Ω. S_{21} parameter magnitude change with frequency analytically calculated and found in simulations over the range spanning from 100 MHz to 5 GHz is shown in Fig. 6. Also, focused views of the S_{21} parameter magnitude change plots throughout the band between 1.7 GHz and 2.3 GHz are shown in the inset figure. It is seen that in the calculations the maximum S_{21} magnitude value of -0.003 dB is achieved at 1.97 GHz and in the simulations the maximum S_{21} magnitude of -3.04 dB is attained at 1.98 GHz. The variation in the peak S_{21} magnitude values is because of the fact that in the theoretical analysis microstrip lines are assumed to be lossless but in the simulations material losses of the copper layers and FR4 substrate are taken into account. On the other hand, the frequencies at which the maximum S_{21} magnitude values are reached are almost the same. Very small variation of 10 MHz might be due to the finite precision of the calculations and limited accuracy of the simulations. Additionally, the filter's -3 dB bandwidth is found to be 210 MHz, i.e., S_{21} magnitude values higher than or equal to -3.003 dB between 1.87 GHz and 2.08 GHz, in the calculations and 190 MHz, such that S_{21} magnitude values are above -6.04 dB between 1.90 GHz and 2.09 GHz, in the simulations, respectively. Very small shifts between the results are again because of the finite precision of the calculations and limited accuracy of the simulations. Moreover, as seen in the figure the S_{21} parameter changes analytically calculated and found in the simulations are very similar outside the interested frequency band, too. Agreement between the results obtained with the theoretical analysis and simulations is expected, which demonstrates the correctness of the found results.

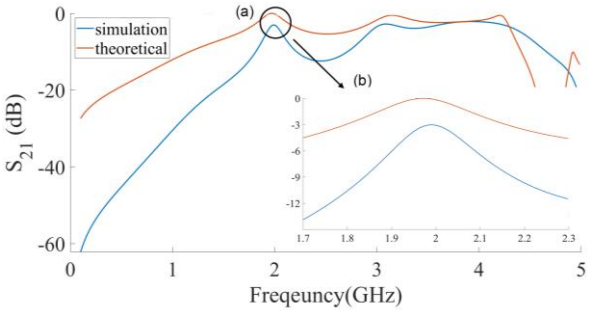

Figure 6. S_{21} parameter of the initially designed filter with no additional via around the microstrip lines analytically calculated and found in the simulations over the frequency band between (a) 100 MHz and 5 GHz, (b) 1.7 GHz and 2.3 GHz

The simulations were then performed for five different numbers of additional vias that are 12, 24, 36, 48, and 60, around the copper lines. As previously mentioned, the newly inserted vias in these designs are 0.3 mm apart from the closest copper line edges. Fig. 7 displays the S_{21} parameter changes of the filters with extra vias that were computed through the simulations. As in Fig. 6, the inset figure (Fig. 7(b)) shows the change focused on the band between 1.7 GHz and 2.3 GHz, whereas the outer figure (Fig. 7(a)) exhibits the change in the frequency spectrum spanning from 100 MHz to 5 GHz.

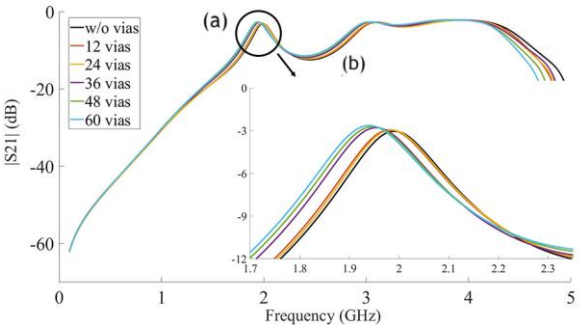

Figure 7. S_{21} parameter of the filters with different numbers of additional vias calculated in the simulations over the frequency band between (a) 100 MHz and 5 GHz, (b) 1.7 GHz and 2.3 GHz

In the figure, it is seen that the maximum S_{21} magnitude value reached in the pass band increases with the number of the additional vias, whereas the frequency at which the maximum S_{21} magnitude is achieved decreases. The S_{21} parameter magnitude was calculated to be -3.026 dB at 1.99 GHz, -2.891 dB at 1.988 GHz, -2.910 dB at 1.983 GHz, -2.752 dB at 1.952 GHz, -2.691 dB at 1.943 GHz, and -2.633 dB at 1.936 GHz in the filter designs without any additional via and with 12, 24, 36, 48, and 60 additional vias, respectively. The increase in the maximum S_{21} magnitude value with the number of vias is expected due to the enhanced encapsulation of the electromagnetic waves while propagating inside the filter. The shift in the frequency, on the other hand, is not expected. In the figure, it is also seen that the -3 dB cut-off frequencies shift to lower frequencies as the number of vias increases. However, the -3 dB bandwidth expands as more vias are placed. The -3 dB bandwidths are found to be 188 MHz, 201 MHz, 197 MHz, 199 MHz, 202 MHz, and 209 MHz, for the filter without any additional via, and with 12, 24, 36, 48, and 60 vias, respectively. For clarity, all these values found for the designed filters with different numbers of additional vias are tabulated in Table 2.

Table 2. Results of the designed filters with different numbers of vias

# of additional vias	Maximum S_{21} magnitude value (dB)	Maximum S_{21} Frequency (GHz)	-3 dB Bandwidth (MHz)
0	-3.026	1.990	188
12	-2.891	1.988	201
24	-2.910	1.983	197
36	-2.752	1.952	199
48	-2.691	1.943	202
60	-2.633	1.936	209

After, simulations were obtained with the designed filter having 60 additional vias around the microstrip lines for different distances between the vias and the lines. In other words, the simulations performed lastly in the via number analysis were repeated by moving the vias closer to and away from the microstrip lines. Since the number of the vias is not changed, the distance between the consecutive additional vias is constant such that the separation between the centers of two horizontal (or vertical) consecutive vias is 2.8 mm. S_{21} parameter magnitude changes calculated in the simulations for the designed filters with varying distances between the vias and microstrip lines are shown in Fig. 8. As in the above figures, i.e., Fig. 6 and Fig. 7, here S_{21} parameter magnitude change with frequency over the band spanning from 100 MHz to 5 GHz is shown in the outside figure (see Fig. 8(a)) and the change zoomed in over the band between 1.7 GHz and 2.2 GHz is illustrated in the inset (see Fig. 8(b)).

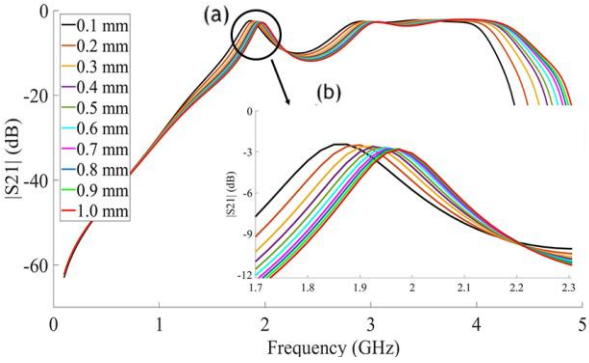

Figure 8. S_{21} parameter of the filter with different distances between the vias and the microstrip lines calculated in the simulations over the frequency band between (a) 100 MHz and 5 GHz, (b) 1.7 GHz and 2.3 GHz

In the figure it is seen that as the distance between the vias and the microstrip lines increases the maximum S_{21} magnitude value in the pass band region of the filter decreases and the frequency at which the maximum S_{21} magnitude is observed shifts to higher frequencies. The decrease of the peak S_{21} magnitude with the distance is expected and it is explained with the reduced encasement of the waves inside the filter as the vias move away from the microstrip lines. In addition, shift of the frequency at which the peak S_{21} magnitude is achieved with the via distance is similar to the shift of the frequency with the via number observed before in the analysis. Guidance of the waves becomes stronger with both increase of the via number and decrease of the via distances to the microstrip lines. Therefore, the frequency at which the maximum S_{21} parameter value is reached shifts to lower frequencies as the via number increases or distances between the vias and the microstrip lines decrease. In the figure, it is also seen that the -3 dB cut-off frequencies of the band shift to lower frequencies as the vias get closer to the microstrip lines. Moreover, the -3 dB bandwidth of the filter has a decreasing trend as the distance between the vias and the microstrip lines become larger. The -3 dB bandwidth of the filter is found to be 233 MHz, 241 MHz, 207 MHz, and 195 MHz for the separation between the vias and the microstrip lines equals to 0.1 mm, 0.4 mm, 0.7 mm, and 1.0 mm, respectively. As in Table 2, the maximum S_{21} parameter values and corresponding frequencies together with the -3 dB bandwidths found for the filters with various distances between the vias and the microstrip lines are given in Table 3.

Table 3. Results of the designed filters with different distances between the vias and the microstrip lines

Via- line distance (mm)	Maximum S_{21} magnitude value (dB)	Maximum S_{21} Frequency (GHz)	-3 dB Bandwidth (MHz)
0.1	-2.452	1.876	233
0.2	-2.498	1.904	237
0.3	-2.585	1.908	245
0.4	-2.622	1.925	241
0.5	-2.686	1.936	226
0.6	-2.694	1.944	219
0.7	-2.783	1.952	207
0.8	-2.790	1.961	203
0.9	-2.798	1.964	201
1.0	-2.822	1.975	195

4. MEASUREMENTS and SYSTEM EXPERIMENTS

To verify the results obtained in the simulations, the designed filters were produced and their transmission responses were measured. Photos of the manufactured filters without any additional via and with a total number of 60 additional vias around the microstrip lines are shown in Fig. 9. The filter without any additional via was produced to have the same geometry as the initially designed and simulated filter. As seen in Fig. 9(a), there are five stubs ended with shorting vias. These vias were filled with a solder to make a connection to the bottom ground plate. Similarly, the second filter, whose photo is shown in Fig. 9(b), was manufactured to have the geometry same with the filter simulated before. As seen in the figure, there are 60 additional vias placed around the microstrip lines. These vias have a cylindrical geometry with a circular cross section having a diameter of 1.4 mm approximately. As in the shorting vias exist at the end of the stubs, the additional vias were also filled with solder and they are in contact with the bottom ground plate.

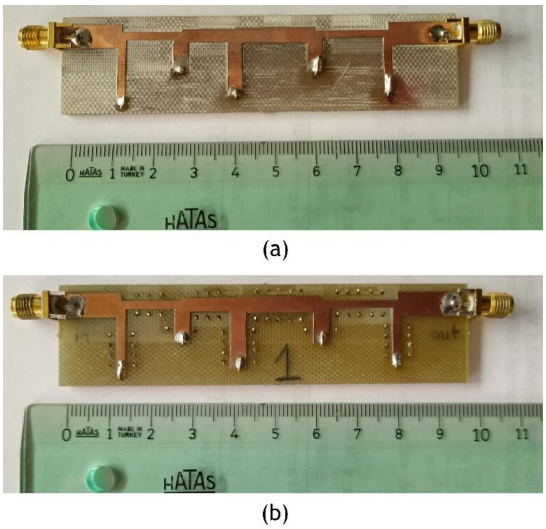

Figure 9. The manufactured filters (a) without any additional via and (b) with 60 additional vias placed around the microstrip lines, where the distance between the centers of the added vias and the copper lines is 1.0 mm

With a network analyzer, S_{21} parameters of the filters were measured. For comparison purpose, in Fig. 10 measured S_{21} parameter magnitude changes over the frequency band between 100 MHz and 5 GHz are represented together with the simulation results. As in the above figures, here in the inset changes of the S_{21} parameter magnitude focused over the frequency band between 1.7 GHz and 2.3 GHz are plotted.

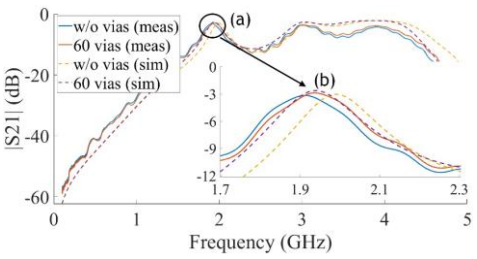

Figure 10. S_{21} parameter magnitude changes of the designed filters obtained in measurements and calculated in simulations over the frequency band between (a) 100 MHz and 5 GHz, (b) 1.7 GHz and 2.3 GHz

In the figure it is seen that the measurement and simulation results agree well. The small differences are due to manufacturing and simulation errors. On the other hand, it is also observed from the measurement results that the peak S_{21} parameter magnitude value inside the pass band of the filter is higher in the case of with additional vias then that reached in the filter design without any additional via. This observation is expected and it is the same with that seen in the simulations. Here, thanks to the additional vias placed around the microstrip lines the maximum S_{21} magnitude achieved in the pass band of the filter increases by 0.4 dB in measurements.

Following the fabrication and measurements of the filter response with the network analyzer, system experiments were performed. To this end, a receiver system setup operating at 1.93 GHz in 2G frequency band was constructed. In the system, an omnidirectional monopole antenna is used and the signal received by the antenna is first amplified with an amplifier and then filtered out with the designed filters. To model a GSM signal in the transmitter side another monopole antenna that is exactly the same with the antenna used in the receiver side is connected to the output of a waveform signal generator. During the experiments a sinusoidal signal at 1.93 GHz was generated from the signal generator and radiated from the transmitter antenna. These signals were received by the receiver antenna, and after amplification and filtering the signals were recorded by means of a spectrum analyzer. The constructed system setup is shown in Fig. 11.

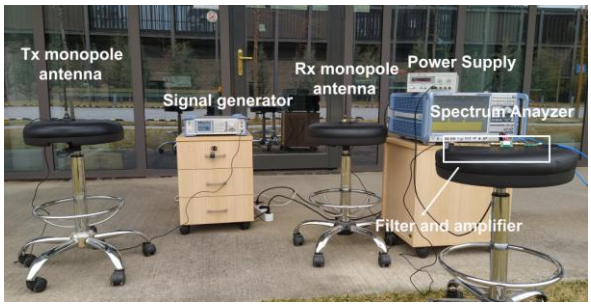

Figure 11. Image of the system setup built in during experiments and the system parts

The experiments were repeated with both of the manufactured filters, i.e., the filter without any additional via and the filter with 60 vias around the microstrip lines, one by one.

The received signals recorded by the spectrum analyzer are shown in Fig. 12. As expected, the signal level at 1.93 GHz frequency is high when the filter with additional vias is used instead of the filter without any additional via. In other words, the loss in the pass band of the filter is decreased, which enables high signal quality, in a system with the designed filter having additional vias around the microstrip lines.

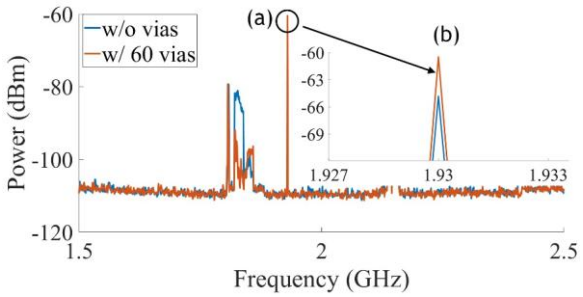

Figure 12. Signals received by the constructed system and recorded by the spectrum analyzer. (a) Over the frequency band between 1.5 GHz and 2.5 GHz, (b) focused view of the signals at 1.93 GHz

In addition, in the figure it is also seen that the unwanted signals outside the 1.93 GHz band are suppressed more when the filter with additional vias is used. This also increases quality of the system signal carrying information at 1.93 GHz GSM band. In the figure it is observed that the measured signal level at 1.93 GHz is increased by more than 4 dB, i.e., from -64.81 dB to -60.47 dB, (see Fig. (12b)) and the unwanted signal level at 1.825 GHz is decreased by approximately -13 dB (from -81.52 dB to -94.91 dB) (see Fig. 12(a)).

Finally, the characteristics of the designed and manufactured bandpass filter are compared with those of the narrow band microstrip band pass filters operating at and around 1.93 GHz available in literature. The results are given in Table 4.

It is seen from the table that the FBW of the designed filter is higher than that of the literature studies. In addition, minimum insertion loss of our filter is a bit lower than those reported in [60-63] but still comparable. Also, the same is true for the filter sizes. These are drawbacks of the filter that we designed and mainly due to the used substrate material. Except the filter specified in [61] and our work, in the other filters materials other than low cost FR4 dielectric are used. In [62] the substrate material is not defined but in [60] and [63] Rodgers and CER-10 Teflon materials, which are more expensive with respect to FR4, are used. The low cost is one of the advantages of our designed filter. Moreover, it is seen that the minimum insertion loss of our designed filter is approximately 4 dB higher than that of the filter given in [61]. This is another advantage of the proposed filter. As explained above, with the designed structure electromagnetic waves are encapsulated more while they are propagating inside the filter, which decreases losses. Furthermore, the suppression level of the designed filter is very similar to those given in [62] and [63].

Table 4. Comparisons of the microstrip bandpass filters

	f_c (GHz)	Pass-band 3dB FBW (%)	Min IL (dB)	Stop-band suppression level	Package Size (mmxmm)	Substrate material and cost
[60]	2	5.9	-2.85	Not defined for 10 dB (but >27 dB up to 2.88 f_c)	45.4x35.6	Rodgers – high cost
[61]	1.8	5.6	-6.983	Not defined	21.0x102.2	FR4 – low cost
[62]	1.8	8.33	≈-2.5	>10 dB below ≈0.92 f_c and above ≈1.06 f_c	≈27.0x22.0	Not defined
[63]	1.655	2	-2.49	>10 dB below ≈0.89 f_c and above ≈1.14 f_c	≈45.0x.57.0	CER-10 Teflon – high cost
Our work	**1.93**	**10.36**	**-3**	**>10 dB below 0.92 f_c and above 1.14 f_c**	**25.0x100.0**	**FR4 – low cost**

*f_c, FBW, and IL stand for pass band center frequency, fractional bandwidth, and insertion loss, respectively. Also, '≈' sign represents that the values are approximate obtained from given figures in the papers, etc.

5. CONCLUSION

In this study, an improved performance microstrip filter with a pass band around the GSM frequency of 1.93 GHz is constructed. The designed filter consists of 5 microstrip stubs ended with vias shorted to the ground and 6 other microstrip lines that are between the stubs and at the input and the output. Initially, the filter was designed and modeled without any vias except the shorting vias at the end of the stubs by means of an electromagnetic solver and after that additional vias were added around the strip lines to increase the filter performance. The simulations were performed with the designed filter for different number of vias around the lines. It is observed that the maximum S_{21} magnitude value reached in the pass band increases with the number of vias, whereas the frequency at which the maximum S_{21} value is achieved decreases. In the simulations the maximum S_{21} magnitude value of the designed filter achieved in the pass band was calculated to be -3.026 dB at 1.99 GHz, -2.891 dB at 1.988 GHz, -2.910 dB at 1.983 GHz, -2.752 dB at 1.952 GHz, -2.691 dB at 1.943 GHz, and -2.633 dB at 1.936 GHz, for the cases without any additional via and with 12, 24, 36, 48, and 60 additional vias, respectively. In addition, from the results it is also seen that the -3 dB cut-off frequencies of the filter shift to lower frequencies while the -3 dB bandwidth expands as more vias are placed around the lines.

After filter analysis with different numbers of additional vias around the lines, simulations were obtained for the designed filter with vias around the lines located at different distances away from the lines. For the filter with 60 additional vias around the microstrip lines simulations were repeated with distances varying from 0.1 mm till 1.0 mm. Results show that the peak S_{21} magnitude value reached in the pass band of the filter gets lower while the frequency at which the maximum S_{21} magnitude is obtained shifts to higher frequencies as the distance between the vias and the microstrip lines increases. This behavior is the same with what was observed in via number analysis and can be explained with encasement of the wave. As the number of the vias increase and the vias get closer to the microstrip lines waves are encapsulated more in the filter. In the simulations it is found that the -3 dB cut-off frequencies of the designed filter shift to lower frequencies as the vias get closer to the microstrip lines. In addition, the -3 dB bandwidth of the filter has a decreasing trend with the increase of the distance between the vias and the microstrip lines.

Next, the designed filters without any additional vias and with 60 additional vias around the lines having 1.0 mm distance were manufactured and their S_{21} parameters were measured. Both the simulation and measurement results are in good agreement. In addition, a simple receiver system setup operating at 1.93 GHz GSM frequency band was constructed. Experiments were performed with the constructed system for the manufactured filters one by one and the received signals in each case were recorded by using a spectrum analyzer. The signal level at 1.93 GHz frequency is observed to be higher for the system in which the designed filter with 60 vias is used than for the system in which the filter without any additional via is used. In addition, in the experiments it was measured that the unwanted signals outside the 1.93 GHz band are suppressed more when the filter with additional vias is used instead of the filter without any additional via. These results demonstrate that signal-to-noise ratio (SNR) of the signal received by the constructed system is increased more with the designed filter having additional vias around the microstrip lines.

Comparisons of the designed filter with narrow band microstrip band pass filters operating at and around 1.93 GHz available in literature show that the designed filter has bandwidth, minimum insertion and stop band suppression level values comparable with those of the filters reported in literature despite it is made of a low cost FR4 dielectric substrate material. The designed filter has 1.93 GHz pass band center frequency (f_c),

10.36% pass band 3 dB FBW, -3 dB minimum insertion loss in the pass band, and stop band suppression level of bigger than 10 dB at frequencies below 0.89 f_c and above 1.14 f_c. The filter is made of low cost FR4 dielectric substrate material and it has 25x100 mm^2 total package size. The features of the designed filter including its size, FBW and suppression level can be enhanced further but it is important to note that the insertion loss of the filter is approximately 4 dB higher than that of another filter reported in literature, which is made of the same FR4 dielectric material. In future studies, a part of the filter can be bent or rotated to create a more compact geometry.

We believe that the proposed filter architecture inspired by SIW structure is beneficial for applications in which low loss in the pass band and high suppression in the outside bands, in other words high signal-to-noise ratio, are required such as 2G, 3G, 4G, 5G GSM communication systems, radar receiver systems, space communication systems, etc.

DECLARATION OF ETHICAL STANDARDS

The authors of this article declare that the materials and methods used in their studies do not require ethical committee approval and/or legal-specific permission.

AUTHORS' CONTRIBUTIONS

Hüseyin TOSUN: Conducting experiments, finalizing simulations, analyzing results and writing the manuscript.

Abdulkadir YENTÜR: Performing simulations, conducting early stage experiments and analyzing results.

Veli Tayfun KILIÇ: Analyzing the results, making analytical calculations, reviewing and editing the manuscript.

CONFLICT OF INTEREST

There is no conflict of interest in this study.

REFERENCES

[1] Nilsson J.W. and Riedel S.A., "***Active Filter Circuits***", Prentice Hall, New Jersey, USA, (2011).

[2] Mabrouk M., Abderrahim B., Djeriri Y., Ameur A. and Bessas A., "Design of a standalone hybrid power system and optimization control with intelligent MPPT algorithms", ***Journal of Polytechnic***, 27(1): 153–167, (2024).

[3] Pozar D.M., "***Microwave Engineering***", Wiley, New York, USA, (2005).

[4] Hong J.-S. and Lancaster M.J., "***Microstrip Filters for RF/Microwave Applications***", Wiley, New York, USA, (2001).

[5] Yang B., Mehdi G., Hu A., Xie Y., Yao X., Zhang J., Zheng C. and Miao J., "The round-ended design and measurement of all symmetric edge-coupled bandpass filter", ***Progress in Electromagnetics Research***, 38: 191–203, (2013).

[6] Yang B., Mehdi G., Zhang J., Yu T., Yao X. and Miao J., "The compact microstrip bandstop filter using equal width open stub", ***International Conference on Green Computing and Communications and IEEE Internet of Things and IEEE Cyber, Physical and Social Computing***, Beijing, China, 1622-1625, (2013).

[7] Seven Z.S. and Can S., "Genetic algorithm and particle swarm optimization approach for prediction of physical parameters of rectangular-shaped microstrip antenna", ***Journal of Polytechnic***, 27(2): 777–787, (2024).

[8] Khateb F., Prommee P. and Kulej T., "MIOTA-based filters for noise and motion artifact reductions in biosignal acquisition", ***IEEE Access***, 10: 14325–14338, (2022).

[9] Aydogan I. and Akman Aydin E., "Wearable electromyogram design for finger movements based real-time human-machine interfaces", ***Journal of Polytechnic***, 26(2): 973–981, (2023).

[10] Mukherjee S., Mutnury B., Dalmia S. and Swaminathan M., "Layout-level synthesis of RF inductors and filters in LCP substrates for Wi-Fi applications", ***IEEE Transactions on Microwave Theory and Techniques***, 53(6): 2196–2210, (2005).

[11] Golestanifar A., Karimi G. and Lalbakhsh A., "Varactor-tuned wideband band-pass filter for 5G NR frequency bands n77, n79 and 5G Wi-Fi", ***Scientific Reports***, 12: 16330(1) –16330(10), (2022).

[12] Doumanis E., Goussetis G. and Kosmopoulos S., "***Filter Design for Satellite Communications: Helical Resonator Technology***", Artech House, MA, USA, (2015).

[13] Yu M., Tang W.-C., Malarky A., Dokas V., Cameron R. and Wang Y., "Predistortion technique for cross-coupled filters and its application to satellite communication systems", ***IEEE Transactions on Microwave Theory and Techniques***, 51(12): 2505–2515, (2003).

[14] Lalbakhsh A., Jamshidi M., Siahkamari H., Ghaderi A., Golestanifar A., Linhart R., Talla J., Simorangkir R.B.V.B. and Mandal K., "A compact lowpass filter for satellite communication systems based on transfer function analysis", ***AEU International Journal of Electronics and Communications***, 124: 153318(1)–153318(7), (2020).

[15] Lalbakhsh A., Mohamadpour G., Roshani S., Ami M., Roshani S., Sayem A.S., Alibakhshikenari M. and Koziel A.S., "Design of a compact planar transmission line for miniaturized rat-race coupler with harmonics suppression", ***IEEE Access***, 9: 129207–129217, (2021).

[16] Yan W.S.T., Mak R.K.C. and Luong H.C., "2-V 0.8-/spl mu/M CMOS monolithic RF filter for GSM receivers", ***IEEE MTT-S International Microwave Symposium Digest (Cat. No.99CH36282)***, Anaheim, CA, USA, 569-572, (1999).

[17] Proakis J.G. and Salehi M., "***Communication Systems Engineering***", Prentice Hall, New Jersey, USA, (2001).

[18] Mustari N., Karabulut M.A., Shah A.F.M.S and Tureli U., "1G'den 6G'ye hücresel evrim üzerine kapsamlı bir derleme", ***Journal of Polytechnic***, 28(2): 351–371, (2025).

[19] GSMA, "Legacy mobile network rationalisation: Experiences of 2G and 3G migrations in asia pacific," https://www.gsma.com/connectivity-for-good/spectrum/wp-content/uploads/2020/06/Legacy-mobile-network-rationalisation.pdf, GSMA, London, UK, (2020).

[20] Stanivuk V., "Measurements of the GSM signal strength by mobile phone", ***20th Telecommunications Forum***, Belgrade, Serbia, 1784-1787, (2012).

[21] Li X., Wang S. and An W., "Design of Tri-Band Dual-Polarized Base Station Antenna for 2G/3G/4G/5G", ***Wireless Networks***, 30: 1633–1642, (2024).

[22] Feng B., Qi S., Ding X., Yang X. and Sim C.-Y.-D., "A dual-polarized multi-wideband ceiling antenna with eight-diagram shape for 2G/3G/LTE/5G sub-6 GHz indoor applications", ***IEEE Access***, 12: 135338–135351, (2024).

[23] Patel D.H. and Makwana G.D., "Multiband antenna for 2G/3G/4G and sub-6 GHz 5G applications using characteristic mode analysis", ***Progress In Electromagnetics Research M***, 115: 107–117, (2023).

[24] Khan A., Ahmad A. and Alam M., "A high-gain reflector-DGS-superstates -enabled quad-band 5G-antenna for mm-wave applications", ***Transactions on Electromagnetic Spectrum***, 3(1): 34–50, (2023).

[25] Poddar H., Ju S., Shakya D. and Rappaport T.S., "A tutorial on NYUSIM: Sub-terahertz and millimeter-wave channel simulator for 5G, 6G, and beyond", ***IEEE Communications Surveys & Tutorials***, 26(2): 824–857, (2024).

[26] Rubio L., Penarrocha V.M.R., Cabedo-Fabres M., Bernardo-Clemente B., Reig J., Fernandez H., Perez J. R., Torres R.P., Valle L. and Fernandez O., "Millimeter-wave channel measurements and path loss characterization in a typical indoor office environment", ***Electronics***, 12(4): 844, (2023).

[27] Babarinde I.O., Ojo J.S. and Ajewole M.O., "High-capacity millimeter wave channel for 5G and future generation systems deployment in tropical region using NYUSIM algorithm", ***Transactions on Electromagnetic Spectrum***, 3(1): 1–19, (2024).

[28] Hribšek M.F., Tošić D.V., Tasić M., Filipović Z. and Živković Z., "Design and realization of transversal surface acoustic wave RF filters", ***Proceedings of Papers 5th European Conference on Circuits and Systems for Communications***, Belgrade, Serbia, 82-85, (2010).

[29] Chen P., Li G. and Zhu Z., "Development and application of SAW filter", ***Micromachines***, 13(5): 656(1)–656(15), (2022).

[30] Anwar M.S. and Dhanyal H.R., "Design of S-band combline coaxial cavity bandpass filter", ***15th International Bhurban Conference on Applied Sciences and Technology (IBCAST)***, Islamabad, Pakistan, 866-869, (2018).

[31] Tomassoni C., Bastioli S. and Sorrentino R., "Generalized TM dual-mode cavity filters", ***IEEE Transactions on Microwave Theory and Techniques***, 59(12): 3338–3346, (2011).

[32] Yassini B., Yu M. and Keats B., "A Ka -band fully tunable cavity filter", ***IEEE Transactions on Microwave Theory and Techniques***, 60(12): 4002–4012, (2012).

[33] Garcia R.G., Renedo M.S., Jarry B., Lintignat J. and Barelaud B., "A class of microwave transversal signal-interference dual-passband planar filters", ***IEEE Microwave and Wireless Components Letters***, 19(3): 158–160, (2009).

[34] Lalbakhsh A., Karimi G. and Sabaghi F., "Triple mode spiral wideband bandpass filter using symmetric dual-line coupling", ***Electronics Letters***, 53(12): 795–797, (2017).

[35] Karimi G., Lalbakhsh A., Dehghani K. and Siahkamari H., "Analysis of novel approach to design of ultra-wide stopband microstrip low-pass filter using modified U-shaped resonator", ***ETRI Journal***, 37(5): 945–950, (2015).

[36] Bai J. and Li L., "Mode-selective corrugated substrate integrated waveguide: A new SIW transmission line : Design a new mode-selective transmission line", ***International Applied Computational Electromagnetics Society Symposium***, Beijing, China, 1-2, (2018).

[37] Wu K., Bozzi M. and Fonseca N.J.G., "Substrate integrated transmission lines: Review and applications", ***IEEE Journal of Microwaves***, 1(1): 345–363, (2021).

[38] Parment F., Ghiotto A., Vuong T.-P., Duchamp J.-M. and Wu K., "Air-filled SIW transmission line and phase shifter for high-performance and low-cost U-Band integrated circuits and systems", ***Global Symposium on Millimeter-Waves (GSMM)***, Montreal, QC, Canada, 1-3, (2015).

[39] Alam A., Alam M.S., Almuhanna K., Zhang H., Shamim A. and Shamsan Z.A., "A wideband transition design technique from RWG to SIW technologies", ***IEEE Access***, 11: 109539–109552, (2023).

[40] Liu Z. and Xiao G., "Design of SIW-based multi-aperture couplers using ray tracing method", ***IEEE Transactions on Components, Packaging and Manufacturing Technology***, 7(1): 106–113, (2017).

[41] Chen J.-X., Hong W., Hao Z.-C., Li H. and Wu K., "Development of a low cost microwave mixer using a broad-band substrate integrated waveguide (SIW) coupler", ***IEEE Microwave and Wireless Components Letters***, 16(2): 84–86, (2006).

[42] Abedi H., Taskhiri M.M. and Hadian E., "Design and analysis of multi-layer SIW coupler to use in phased array antenna feed network", ***The Journal of Engineering***, 3: 1–8, (2023).

[43] Wu Z.-M., Ji L., Li X.-C., Zhu H.-B and Mao J.-F., "A slow wave folded ridge HMSIW using spoof surface plasmon polaritons structure and its application in coupler design", ***IEEE Transactions on Components, Packaging and Manufacturing Technology***, 13(5): 594–603, (2023).

[44] Bilawal F., Babaeian F., Trinh K.T. and Karmakar N.C., "The art of substrate-integrated-waveguide power dividers", ***IEEE Access***, 11: 9311–9325, (2023).

[45] Khan A.A. and Mandal M.K., "Miniaturized substrate integrated waveguide (SIW) power dividers", ***IEEE Microwave and Wireless Components Letters***, 26(11): 888–890, (2016).

[46] Hao Z., Hong W., Li H., Zhang H. and Wu K., "Multiway broadband substrate integrated waveguide

(SIW) power divider", ***IEEE Antennas and Propagation Society International Symposium***, Washington, DC, USA, 639-642, (2005).

[47] Chen S.Y., Zhang D.S. and Yu Y.T., "Wideband SIW power divider with improved out-of-band rejection", ***Electronics Letters***, 49(15): 943–944, (2013).

[48] Tan L.-R., Wu R.-X. and Poo Y., "Magnetically reconfigurable SIW antenna with tunable frequencies and polarizations", ***IEEE Transactions on Antennas and Propagation***, 63(6): 2772–2776, (2015).

[49] Chaturvedi D. and Raghavan S., "Circular quarter-mode SIW antenna for WBAN application", ***IETE Journal of Research***, 64(4): 482–488, (2018).

[50] Serhsouh I., Himdi M., Lebbar H. and Vettikalladi H., "Reconfigurable SIW antenna for fixed frequency beam scanning and 5G applications", ***IEEE Access***, 8: 60084–60089, (2020).

[51] Chen H., Shao Y., Zhang Y., Zhang C. and Zhang Z., "A millimeter-wave triple-band SIW antenna with dual-sense circular polarization", ***IEEE Transactions on Antennas and Propagation***, 68(12): 8162–8167, (2020).

[52] Vala A. and Patel A., "Half-mode substrate-integrated waveguide based band-pass filter for C band application", ***Microwave and Optical Technology Letters***, 61(6): 1468–1472, (2019).

[53] Wang Y., Hong W., Dong Y., Liu B., Tang H.J., Chen J., Yin X. and Wu K., "Half mode substrate integrated waveguide (HMSIW) bandpass filter", ***IEEE Microwave and Wireless Components Letters***, 17(4): 265–267, (2007).

[54] Garg S. and Raj R.K., "A novel bandpass substrate integrated waveguide filter for the application at K & Ka band", ***International Journal of Research and Analytical Reviews***, 6(1): 1098–1102, (2019).

[55] Moitra S. and Bhowmik P.S., "Design and analysis of 150° bend SIW and corrugated SIW bandpass filter with multiple transmission zeroes using reactive periodic structures suitable for microwave integrated circuits (MICs)", ***Wireless Personal Communication***, 101(1): 167–180, (2018).

[56] Zhao L., Li Y., Chen Z.-M., Liang X.-H., Wang J., Shen X. and Zhang Q., "A band-pass filter based on half-mode substrate integrated waveguide and spoof surface plasmon polaritons", ***Scientific Reports***, 9(1), (2019).

[57] Zhu Y and Dong Y., "A novel compact wide-stopband filter with hybrid structure by combining SIW and microstrip technologies", ***IEEE Microwave and Wireless Components Letters***, 31(7): 841–844, (2021).

[58] Guvenli K., Yenikaya S. and Secmen M., "Analysis, design, and actual fabrication of a hybrid microstrip-SIW bandpass filter based on cascaded hardware integration at X-Band", ***Elektronika IR Elektrotechnica***, 27(1): 23–28, (2021).

[59] Cansever C., "***Design of a Microstrip Bandpass Filter for 3.1–10.6 GHz Uwb Systems***" MS Thesis, Electrical Engineering and Computer Science, Syracuse University, New York, (2013).

[60] Deng P.-A. and Tsai J.-T., "Design of microstrip cross-coupled bandpass filter with multiple independent designable transmission zeros using branch-line", ***IEEE Microwave and Wireless Components Letters***, 23(5): 249–251, (2013).

[61] Mustafa A.T. and Mohammed Ali Y.E., "Designa coupled line microstrip bandpass filter at 1.8 GHz", ***2021 7th International Conference on Advanced Computing and Communication Systems (ICACCS)***, Coimbatore, India, 1437-1441, (2021).

[62] Arunjith K.S., Ghivela G.C. and Sengupta J., "Design and analysis of novel tri-band band pass filter for GSM, WiMax and UWB applications", ***Wireless Personal Communication***, 118: 3457–3467, (2021).

[63] Mao R.-J., Tang X.-H. and Xiao F., "Miniaturized dual-mode ring bandpass filters with patterned ground plane", ***IEEE Transactions on Microwave Theory and Techniques***, 55(7): 1539–1547, (2007).